European Polymer Journal 50 (2014) 168–176

Contents lists available at ScienceDirect

European Polymer Journal

journal homepage: www.elsevier.com/locate/europolj

Complementary multiple hydrogen bonds stabilize thermo-sensitive supramolecular structures prepared from poly(*N*-isopropyl acrylamide) and adenine-functionalized poly(ethylene oxide)

Hui-Wang Cui [a], Wee-Cheng Chu [a], Jem-Kun Chen [b], Shiao-Wei Kuo [a,*]

[a] Department of Materials and Optoelectronic Science, Center for Nanoscience, and Nanotechnology, National Sun Yat-Sen University, 804 Kaohsiung, Taiwan
[b] Department of Materials Science and Engineering, National Taiwan University of Science and Technology, 43, Sec 4, Keelung Road, Taipei 106, Taiwan

ARTICLE INFO

Article history:
Received 28 September 2013
Received in revised form 21 October 2013
Accepted 22 October 2013
Available online 31 October 2013

Keywords:
Supramolecules
Hydrogen bond
Thermo-sensitive polymer
Micomicelles
Viscoelastic properties

ABSTRACT

In this study, we synthesized a poly(*N*-isopropylacrylamide) (PNIPAm) through the polymerization of *N*-isopropylacrylamide in distilled water with azodiisobutyronitrile as the initiator and a bisadenine-functionalized poly(ethylene oxide) (A-PEO-A) from the reaction of adenine with a difunctionalized toluenesulfonyl-PEO. When blended together in distilled water, PNIPAm and A-PEO-A formed supramolecular aggregates stabilized through complementary multiple hydrogen bonds between the amide groups of PNIPAm and the adenine units of A-PEO-A. Fourier transform infrared spectroscopy, ^{1}H nuclear magnetic resonance spectroscopy, transmission electron microscopy, dynamic light scattering, and rheometry revealed the thermo-sensitive behavior and viscoelastic properties of the supramolecular assemblies.

1. Introduction

The properties of stimuli-responsive polymers often vary—sometimes dramatically—to small changes in their environment. Stimuli-responsive changes in shape, surface characteristics, or solubility, or intricate molecular self-assembly or sol–gel transitions, enable several novel applications of such polymers (e.g., the delivery of therapeutics; tissue engineering; cell culturing; bioseparations; sensors or actuators) [1–5]. Poly(*N*-isopropylacrylamide) (PNIPAm), one of the most widely studied thermo-responsive polymers, is soluble in water at temperatures below 32 °C, but precipitates at temperatures above 32 °C. Its phase transition temperature is also referred to as its lower critical solution temperature (LCST). Below the LCST, favorable noncovalent interactions (namely hydrogen bonds between the amide groups in the polymer and water molecules) lead to dissolution of the polymer chains; above the LCST, the hydrogen bonds are broken and water molecules are expelled from the polymer, resulting in its precipitation [6,7]. Therefore, the ability to manipulate the LCST of PNIPAm has been an attractive challenge experimentally and theoretically, with wide potential applicability. Accordingly, various copolymers of PNIPAm have been reported, prepared in conjunction with poly(acrylic acid) [8–13], poly(*N*-vinylpyrrolidone) [12–14], polycaprolactone [15,16], polyacrylate [17], poly(ethylene glycol) methacrylate [18–22], poly[2-(dimethylamino)ethylmethacrylate] [23–26], poly(*N*,*N*-diethylacrylamide) [27], poly(*tert*-butyl acrylate) [13], has been to synthesize copolymers from PNIPAm and PEO—for example, hetero-arm star and double brush-shaped copolymers [28]. The studies mentioned above have mainly used polymerization methods to change or improve the thermo sensitivity and related properties of PNIPAm. A major approach copolymers [17], and H-shaped pentablock copolymers [26]—though

* Corresponding author. Tel.: +886 7 5252000x4079; fax: +886 7 5254099.
E-mail address: kuosw@faculty.nsysu.edu.tw (S.-W. Kuo).

0014-3057/$ - see front matter © 2013 Elsevier Ltd. All rights reserved.
http://dx.doi.org/10.1016/j.eurpolymj.2013.10.023

polymerization methods involving click chemistry [11,16,26,29], ring-opening polymerization [16], atom transfer radical polymerization [16,17,26,29–32], single-electron-transfer living radical polymerization [26], free radical copolymerization [33–36], or reversible addition fragmentation transfer polymerization [37,38]. These approaches usually require a combination of two or more polymerization methods to prepare copolymers exhibiting high performance. Such polymerization methods can, however, be very complex and time-consuming. To avoid these problems, we investigated the use of complementary multiple hydrogen bonding between the amide groups of PNIPAm and adenine (A) units to form supramolecular assemblies through simple blending [4]. In this previous study [4], we only use the low molecular weight adenine with PNIPAm, the hydrogen bonding interaction, and LCST behavior were detail discussed. In this study, we firstly change to synthesize an A-difunctionalized PEO (A-PEO-A) polymers from the reaction of A with a difunctionalized toluenesulfonyl-PEO (Scheme 1(c)) and a PNIPAm from the polymerization of the monomer *N*-isopropylacrylamide (NIPAm). We then mixed PNIPAm with A-PEO-A in distilled water using a simple blending method. The complementary multiple hydrogen bonds formed between the amide groups of PNIPAm and the A units of A-PEO-A led to the development of a supramolecular system in the aqueous solution (Scheme 1(d)). We used Fourier transform infrared (FTIR) spectroscopy, proton nuclear magnetic resonance (^{1}H NMR) spectroscopy, transmission electron microscopy (TEM), dynamic light scattering, and rheometry to investigate the thermo-sensitive behavior and viscoelastic properties of these PNIPAm/A-PEO-A systems.

2. Experiments

2.1. Materials

NIPAm was obtained from Tokyo Chemical Industry (Japan). AIBN, PEO (M_w = 2000) and potassium carbonate (K_2CO_3) were purchased from Showa Chemical. *n*-Butyllithium (*n*-BuLi) in hexane was obtained from Chemetall (Taiwan). *p*-Toluenesulfonyl chloride (TsCl), adenine (A), *N*,*N*-dimethylformamide (DMF), toluene, diethyl ether (Et_2O), dichloromethane (DCM), tetrahydrofuran (THF), and magnesium sulfate ($MgSO_4$) were purchased from Sigma–Aldrich (USA).

2.2. PEO-TsCl

n-BuLi in hexane (12 mL) was injected slowly via syringe into a reactor containing a solution of PEO (25.5 g) in toluene (150 mL) in an ice bath under pure N_2. After the addition was complete, the reactor was kept in the ice bath for 30 min and then a solution of TsCl (8.6 g) in toluene (40 mL) was injected slowly via syringe into the reactor. The mixture was then maintained for 24 h at room temperature. After vacuum distillation of the toluene, the product was dissolved in THF and Et_2O was added

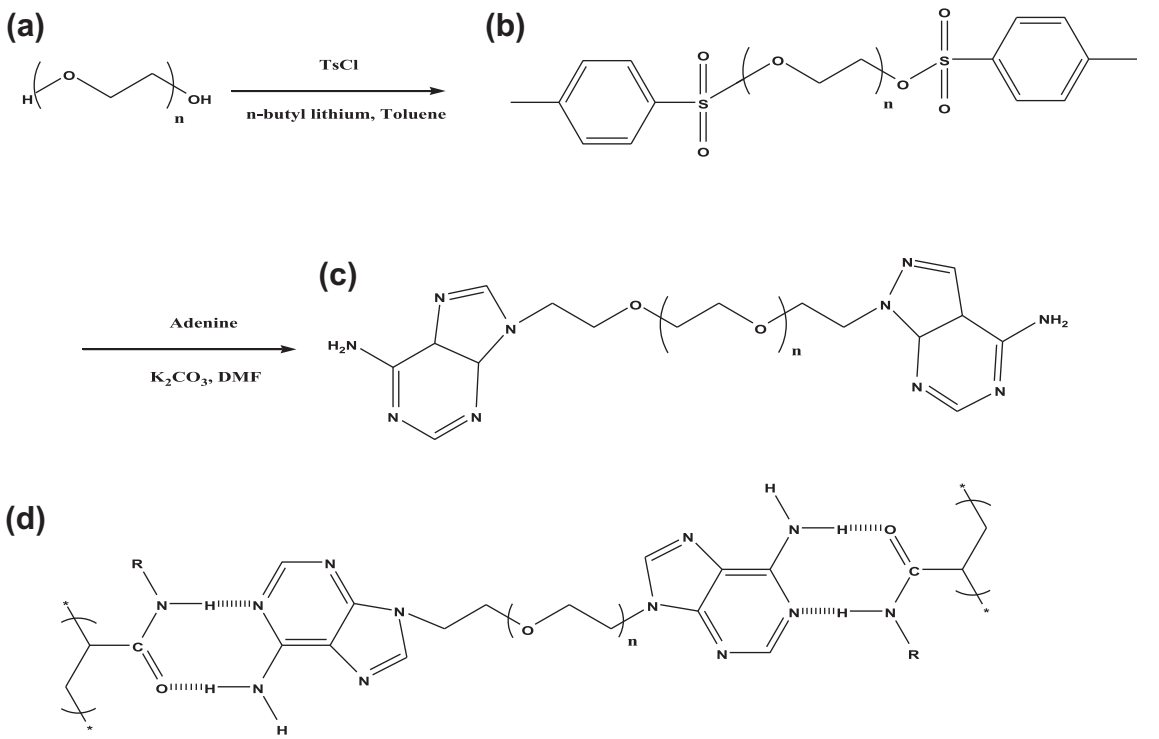

Scheme 1. (a–c) Chemical structures of (a) PEO, (b) TsCl-PEO, and (c) A-PEO-A; (d) multiple hydrogen bonding interactions between the amide groups of PNIPAm and the A groups of A-PEO-A.

dropwise to form a white precipitate. After filtering and drying, a light-yellow powder was obtained (Scheme 1(b)).

2.3. A-PEO-A

Adenine (0.86 g) and K_2CO_3 (0.88 g) were mixed together in a reactor in the solid state under vacuum. After adding anhydrous DMF (50 mL) and changing the reaction surroundings from vacuum state to pure N_2 atmosphere in the reactor, the mixture was stirred vigorously for 4–5 h at room temperature. At this point, a solution of PEO-TsCl (3.68 g) in anhydrous DMF (10 mL) was injected slowly into the reactor via syringe and then the mixture was heated at 70 °C for 12 h. After filtering to remove the precipitate and vacuum distillation to remove the DMF, the product was dissolved in DCM and then filtered again to obtain the filtrate. After drying ($MgSO_4$) and filtering, the solvent was concentrated to provide a light-yellow solution, which was mixed with anhydrous THF to form a precipitate. After filtering, a light-yellow solution was obtained; Et_2O was added dropwise to form light-yellow precipitate. After filtering and drying, a light-yellow powder was obtained (Scheme 1(c)).

2.4. PNIPAm

NIPAm (5 g), AIBN (0.1 g), and distilled water (250 mL) were mixed together for approximately 4 h under pure N_2. After they had dissolved completely, the temperature was increased to 80 °C and the mixture strongly stirred for 12 h at this temperature. After washing monomer sequentially with distilled water and Et_2O, filtering, drying, and grinding, a white crystalline material was obtained.

2.5. PNIPAm/A-PEO-A supramolecular complexes in aqueous solution

PNIPAm (0.01 g, 0.1 mmol) was blended with various amounts of A-PEO-A (see Table 1) in distilled water (10 mL) to form supramolecular complexes stabilized through complementary multiple hydrogen bonding (Scheme 1(d)).

2.6. Characterization

FTIR spectra of the sample pellets were recorded using a Bruker Tensor 27 FTIR spectrophotometer and the conventional KBr disk method; 32 scans were collected at a spectral resolution of 1 cm^{-1}; the pellets used in this study were sufficiently thin to obey the Beer–Lambert law. ^1H NMR spectra of PEO-TsCl, A-PEO-A, and PNIPAm were recorded at room temperature using a Bruker AM 500 (500 MHz) spectrometer, with the residual proton resonance of either D_2O or $CDCl_3$ acting as the internal standard. The ^1H NMR spectra of PNIPAm/A-PEO-A were recorded at temperatures ranging from 25 to 50 °C. The thermo-sensitive behavior of the samples was characterized at temperatures from 25 to 50 °C through static light scattering using a Model DT 1000CE UV/VIS Light Source and a laser wavelength of 680 nm; at each temperature, the solution was equilibrated for 5 min. A mass spectrum was obtained using a Bruker Daltonics Autoflex III MALDI-TOF mass spectrometer. The following voltage parameters were employed: ion source 1, 19.06 kV; ion source 2, 16.61 kV; lens, 8.78 kV; reflector 1, 21.08 kV; reflector 2, 9.73 kV. Transmission electron microscopy (TEM) was performed using a JEOL-2100 transmission electron microscope operated at an accelerating voltage of 200 kV. TEM samples were prepared by dip-coating Cu grids coated with C supporting films into the aqueous solution of PNIPAm/A-PEO-A. The grids were then stained with I_2 for 2 h and left to dry under vacuum at room temperature prior to observation. The hydrodynamic diameters of the assemblies were measured by DLS using a Brookheaven 90 plus model equipment (Brookheaven Instruments Corporation, USA) with a He–Ne laser with a power of 35 mW at 632.8 nm. All DLS measurements were carried out with a wavelength of 632.8 nm at 25 °C with 90° angle of detection. All samples were measured five times and the samples are to filter through 0.45 μm filter before sending it to us for analysis. We analyzed the experimental correlation function using the cumulant method and the CONTIN algorithm. The Stokes–Einstein approximation was used to convert the diffusion coefficient into the form of the hydrodynamic diameter (D_h). The elastic moduli (G') and viscous moduli (G'') of the samples were studied using an Anton Paar Physioa MCR 301 Rheometer at temperatures varied from 25 to 50 °C at a rate of 2 °C min^{-1}; the amplitude (γ) was 0.5% and the angular frequency (ω) was 10 s^{-1}. The apparent viscosities of the samples were also obtained using this rheometer at 25 °C, varied from 2 to 50 s^{-1} at a rate of 0.813 s^{-1} per 5 s.

3. Results and discussion

3.1. Preparation of PNIPAm/A-PEO-A supramolecular systems in aqueous solution

Fig. 1 presents ^1H NMR spectra of PEO-TsCl and A-PEO-A. The signals at 3.71 ppm (peak *a*) in Fig. 1(a)–(c) represents the protons of the OCH_2CH_2 repeating units of PEO. We attribute the signals at 2.41 and 7.71/7.40 ppm in

Table 1
Experimental design of PNIPAm/A-PEO-A supramolecular complexes.

Molar ratio	1:0	1:0.1	1:0.2	1:0.4	1:0.6	1:0.8	1:1	1:1.5	1:2	1:4	0:1
PNIPAm (g)	0.01	0.01	0.01	0.01	0.01	0.01	0.01	0.01	0.01	0.01	–
A-PEO-A (g)	–	0.01	0.02	0.04	0.06	0.08	0.1	0.15	0.2	0.4	0.01
Distilled water (ml)	10	10	10	10	10	10	10	10	10	10	10
Concentration (mg ml^{-1})	1	2	3	5	7	9	11	16	21	41	1

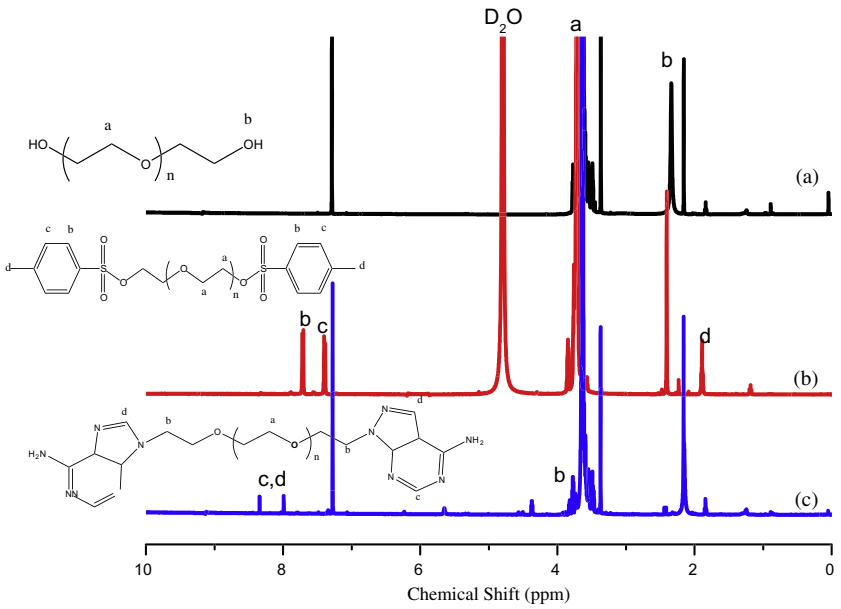

Fig. 1. ^{1}H NMR spectra of (a) pure PEO in $CDCl_3$, (b) PEO-TsCl and (c) A-PEO-A in D_2O.

Fig. 1(b) to the protons of the methyl groups and benzene rings, respectively, of the tosyl units. Those peaks were absent from the spectrum of A-PEO-A in Fig. 1(c), the complete reaction between PEO-TsCl and A was confirmed, in which can observe signals for —N—CH=N—, —N=CH—N—, and —N=C—CH_3 units at 8.34, 7.98, and 5.65 ppm, respectively. The characteristic signal at 3471 cm^{-1} for the OH groups of PEO was absent and aromatic group at ca. 1600–1650 cm^{-1} was appeared in the FTIR spectrum and benzene group of Ts-PEO-Ts (Fig. S1(b)). The corresponding FTIR spectrum features characteristic signal for the NH_2 groups at 3190 and 3385 cm^{-1} for A-PEO-A (Fig. S1(c)). Fig. S2 displays GPC traces of the PEO, and A-PEO-A; all indicate a narrow molecular weight distribution (**<1.1**). The shift to high molecular weight shoulder probably increases molecular weight or due to the polymer-stationary phase interactions arising inter-chain hydrogen bonding of A units. Fig. 2(c) also displays the MALDI-TOF mass of A-PEO-A, indicating also the narrow distribution of A-PEO-A and the molecular weight is ca. 2300, which is close to the prediction molecular weight of A-PEO-A. Taken together, the NMR, FTIR, GPC, and MALDI-TOF mass analyses all confirmed the successful synthesis of A-PEO-A. Fig. S3 shows the ^{1}H NMR spectra (with peaks assignments) of NIPAm monomer and PNIPAm in $CDCl_3$. For NIPAm, signals for the vinyl groups appear at 5.61, 5.04, and 6.25 ppm with a relative ratio of 1:1:1, corresponding to the cis, trans, and substituted vinyl protons, respectively (Fig. S3(a)). These peaks disappeared after polymerization, providing evidence for the complete reaction leading to PNIPAm (Fig. S3(b)). We estimated the molecular weight of PNIPAm by GPC analyses as shown in Fig. S4 (Mn = 50000 g/mol, PDI = 2.03) free radical polymerization.

Fig. 2 displays the transmissions of PNIPAm/A-PEO-A complexes at various molar ratios of PNIPAm and A-PEO-A and the control study of PNIPAm/PEO with hydroxyl group terminated of PEO at the same molecular weight. Upon increasing the molar ratio of A-PEO-A, the concentration of PNIPAm/A-PEO-A in solution increased accordingly, as did the related transmission. In this study, we defined the LCST as the temperature at the half-height of the transmission curve. The LCSTs obtained from the transmission curves in Fig. 2(a) at the various PNIPAm/A-PEO-A molar ratios were 34.8 °C (1:0, pure PNIPAm; 1 mg mL^{-1}), 35.2 °C (1:0.2, 3 mg mL^{-1}), 36.1 °C (1:0.4, 5 mg mL^{-1}), 36.8 °C (1:0.6, 7 mg mL^{-1}), 36.9 °C (1:0.8, 9 mg mL^{-1}), 37.4 °C (1:1, 11 mg mL^{-1}), 38.3 °C (1:1.5, 16 mg mL^{-1}), 39.4 °C (1:2, 21 mg mL^{-1}), and 40.3 °C (1:4, 41 mg mL^{-1}); we could not detect the LCST for pure A-PEO-A (0:1, 1 mg mL^{-1}) within the tested temperature range (25–50 °C). The control study of PNIPAm/PEO without adenine group of PEO shows the two-step transmission decay curves. At lower temperature (ca. 30–35 °C) should be corresponding to LCST for PNIPAm and the higher temperature (ca. 45–50 °C) was corresponding to LCST for PEO as would be expected and this result is quite different with PNIPAm/A-PEO-A. This result should come from two different phase behavior in water of PNIPAm/PEO blend. Therefore, the PNIPAm/A-PEO-A complexes of single phase behavior exhibited reversible thermo-sensitive behavior similar to that of pure PNIPAm (Scheme S1). The LCST of PNIPAm/A-PEO-A increased significantly upon increasing the A-PEO-A content because spherical micelles, large associated aggregates of spherical micelles, network structures, and toroidal structures (Scheme S2) formed as a result of complementary multiple hydrogen bonding between the amide groups of PNIPAm and the A groups of A-PEO-A. Below the LCST, these polymers were hydrophilic, swelling, and soluble, leading to high transmission; above the LCST and at higher solution temperatures, they collapsed, squeezed, and condensed to form hydrophobic, deswelled, insoluble aggregates, thereby exhibiting gel

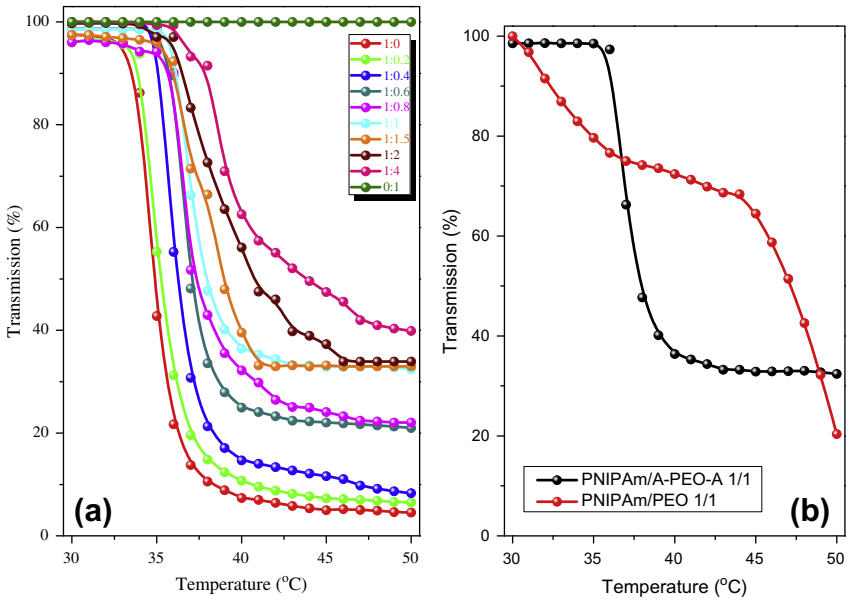

Fig. 2. Transmission of supramolecular complex of (a) PNIPAm/A-PEO-A in aqueous solution with different molar ratios and the control study of (b) PNIPAm/PEO at UV wavelength (λ = 680 nm).

phenomena, becoming cloudy and displaying low transmission.

The thermo-sensitive behavior of the PNIPAm/A-PEO-A complexes was also evidenced by changes in the resonance peaks of the protons in the ^{1}H NMR spectra. Fig. 3 presents ^{1}H NMR spectra of PNIPAm/A-PEO-A supramolecular complexes in D_2O at temperatures from 25 to 50 °C. In each spectrum, the molar ratio of PNIPAm to A-PEO-A was 1:0.1. The ^{1}H NMR spectrum of the PNIPAm/A-PEO-A complex at 25 °C featured signals at 2.03, 1.60, and 1.17 ppm that were clear and sharp, representing the protons of the methylene (CH_2), methine (CH), and methyl (CH_3) groups, respectively, of PNIPAm. At 30 °C, these signals remained clear and sharp. Upon increasing the solution temperature further, these signals became weaker, disappearing completely at 45 and 50 °C. Fig. 4 presents ^{1}H NMR spectra of the PNIPAm/A-PEO-A supramolecular complexes in D_2O at temperatures from 25 to 50 °C. The spectrum of PNIPAm featured a signal at 6.54 ppm,

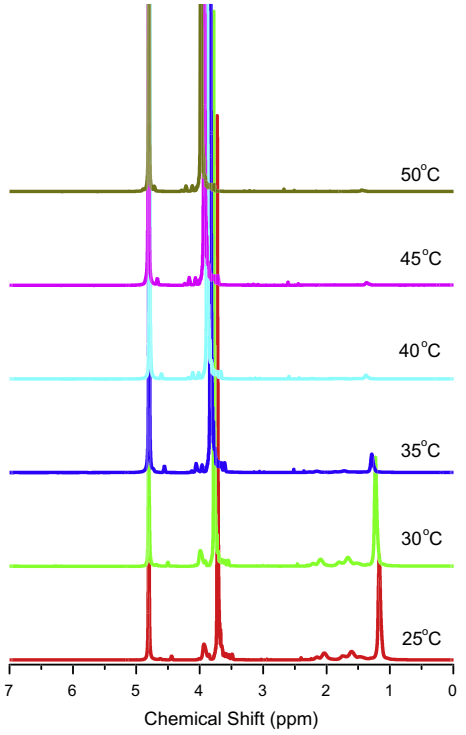

Fig. 3. ^{1}H NMR spectra of PNIPAm/A-PEO-A at a fixed molar ratio of 1:0.1 in D_2O with different temperature.

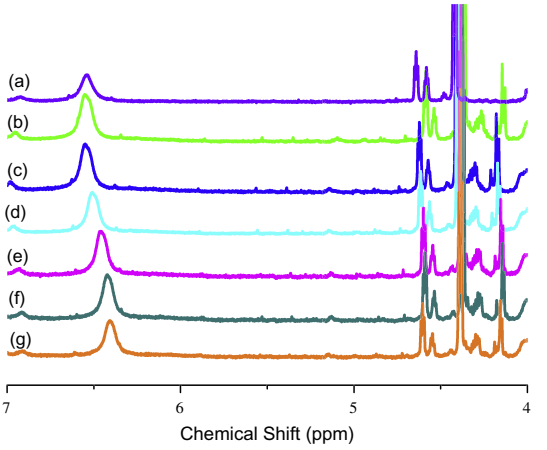

Fig. 4. ^{1}H NMR spectra of (a) pure A-PEO-A at 25 °C and (b–g) PNIPAm/A-PEO-A at a fixed molar ratio (1:4) in D_2O solution.

attributable to the NH groups. Upon increasing the temperature, the spectra of the PNIPAm/A-PEO-A complexes, each at a molar ratio of 1:4, exhibited sharp signals at 6.55 ppm (25 °C), 6.55 ppm (30 °C), 6.51 ppm (35 °C), 6.46 ppm (40 °C), 6.42 ppm (45 °C), and 6.41 ppm (50 °C). These changes in the ^{1}H NMR spectra reflect the presence of complementary multiple hydrogen bonds between the PNIPAm and A-PEO-A components of the complexes.

3.2. Micelle morphology of the PNIPAm/A-PEO-A complexes in aqueous solution

Fig. 5 displays the values of D_H obtained through dynamic light scattering of PNIPAm/A-PEO-A complex in aqueous solution. The values of D_H for PNIPAm and A-PEO-A were both approximately 85 nm; those of the PNIPAm/A-PEO-A mixtures increased as the blend ratio increased: approximately 100 nm (1:0.4, 5 mg mL^{-1}), 125 nm (1:1, 11 mg mL^{-1}), 360 nm (1:2, 21 mg mL^{-1}), and 735 nm (1:4, 41 mg mL^{-1}). Thus, the variation in the values of D_H of the PNIPAm/A-PEO-A systems depended on the molar ratio between PNIPAm and A-PEO-A. In addition, the control study of PNIPAm/PEO without adenine group of PEO (Fig. 5(g)) shows the broader distribution than PNIPAm/A-PEO-A, corresponding to more complex aggregation in water of PNIPAm/PEO blend. The TEM images in solution as they are measured under dry conditions under vacuum were summarized in Figs. S5 and S6.

3.3. Viscoelastic properties of PNIPAm/A-PEO-A supramolecular assemblies in aqueous solution

We used the PNIPAm/A-PEO-A complex formed at a molar ratio of 1:0.1 to determine the apparent viscosity. Because a solution concentration of 2 mg mL^{-1} at this molar ratio was too low to measure the apparent viscosity accurately, we adjusted it to 100 mg mL^{-1}. We determined the apparent viscosities of the PNIPAm and PNIPAm/A-PEO-A systems each at a solution concentration of 100 mg mL^{-1} (Fig. 6). The apparent viscosities of pure PNIPAm (Fig. 6(a)), PNIPAm/A-PEO-A complex (Fig. 6(b)) and PNIPAm/PEO (Fig. 6(c)) blend decreased as the shear rate increased, revealing that both were shear-thinning fluids, also known as pseudoplastic non-Newtonian fluids. The PNIPAm/A-PEO-A complex had a higher apparent viscosity than the pure PNIPAm and PNIPAm/PEO at the same shear rate; the increase in the apparent viscosity resulted from the supramolecular assemblies formed between the amide units in PNIPAm and the A units in A-PEO-A through complementary multiple hydrogen bonding. As revealed in Scheme S2(c) and Figs. S5 and S6, the supramolecular structures that improved the apparent viscosity were

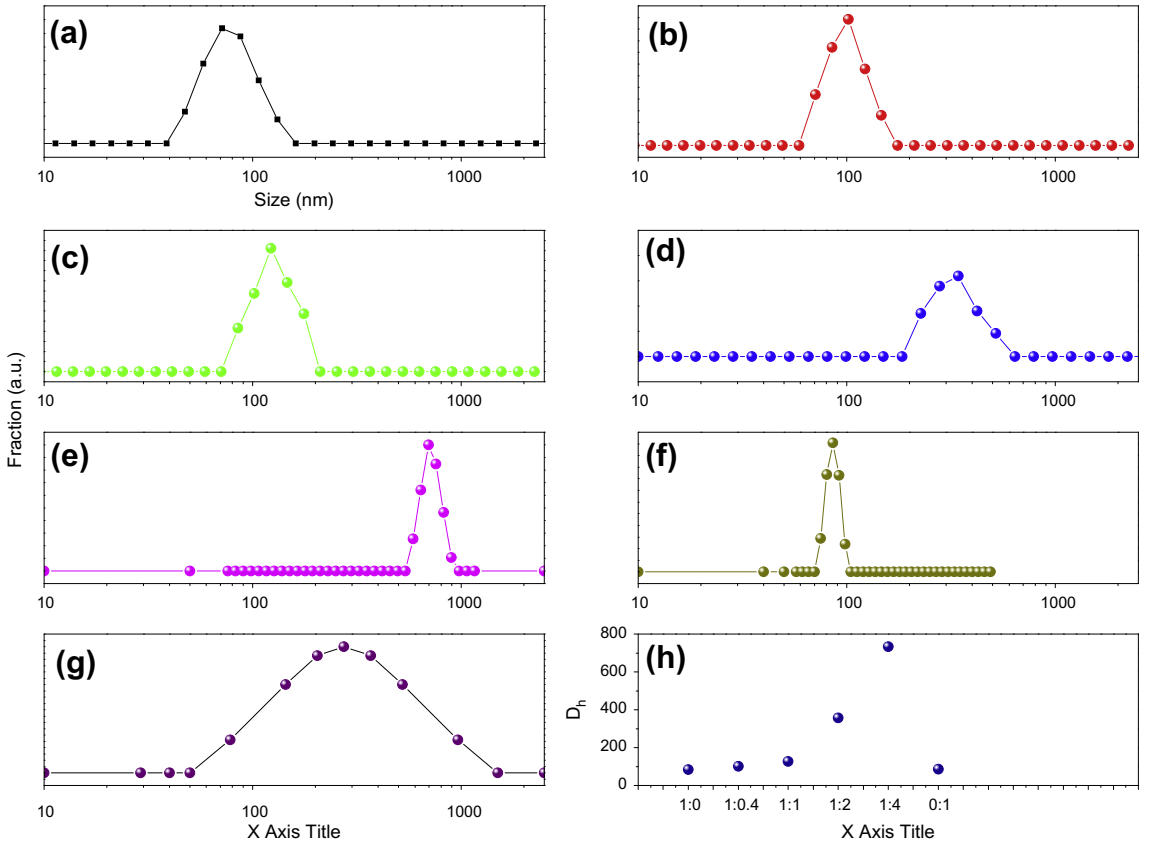

Fig. 5. Particle size distributions in PNIPAm/A-PEO-A blends at molar ratios of (a) 1:0, (b) 1:0.4, (c) 1:1, (d) 1:2, (e) 1:4, (f) 0:1, (g) the control study of PNIPAm/PEO = 1/1, and (h) average values of size distribution of PNIPAm/A-PEO-A.

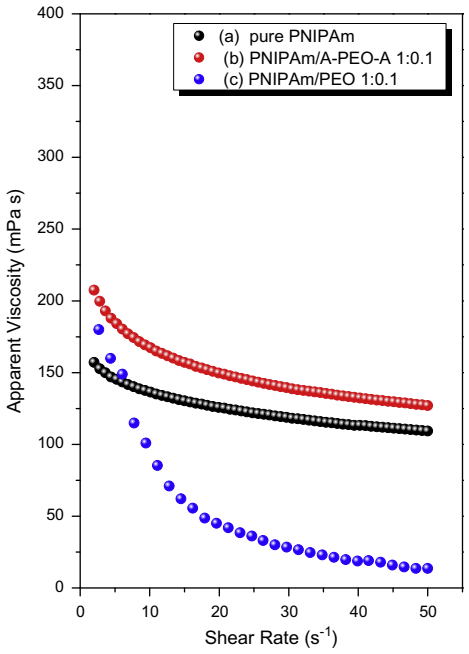

Fig. 6. Apparent viscosities of (a) pure PNIPAm, (b) PNIPAm/A-PEO-A blends at a molar ratio of 1:0.1, and (c) PNIPAm/PEO blends at a molar ratio of 1:0.1.

network-like and toroid structures. To investigate the gel phenomenon visually, we prepared PNIPAm (1:0, 500 mg mL^{-1}) and PNIPAm/A-PEO-A (1:0.1, 500 mg mL^{-1}; 1:1, 500 mg mL^{-1}) systems (Fig. 7(a)). All of these systems exhibited gel phenomena. Although the PNIPAm system exhibited a certain fluidity, the PNIPAm/A-PEO-A complexes did not. The degree of gel formation from the PNIPAm/A-PEO-A complexes was higher than that of the PNIPAm system; that at a molar ratio of 1:1 for PNIPAm/A-PEO-A was greater than that at a molar ratio of 1:0.1.

Moreover, the PNIPAm/A-PEO-A complexes also exhibited good film-forming properties. As Fig. 7(b) reveals, we could prepare films from the PNIPAm/A-PEO-A blend at a molar ratio of 1:1, but not from PNIPAm and A-PEO-A alone because of their high crystallinity and brittleness. These films featured a certain degree of warping, suggesting that they were tough, elastic, and flexible. Thus, the complementary multiple hydrogen bonds formed between the amide units in PNIPAm and the A units in A-PEO-A were responsible for the PNIPAm/A-PEO-A blends exhibiting a high degree of gelation, good toughness, elasticity, and flexibility [39–42].

We further studied the film-forming properties of PNIPAm/A-PEO-A by measuring their elastic modulus (G') and viscous modulus (G''). We prepared solid test samples (Table 2) from PNIPAm/A-PEO-A at molar ratios of 1:0.1, 1:0.4, 1:1, 1:2, and 1:4, as well as pure PNIPAm (1:0) and pure A-PEO-A (0:1). Fig. 8(a) and Table 2 reveal that the value of G' of PNIPAm/A-PEO-A was higher than those for PNIPAm and A-PEO-A; the same trend appears for the values of G'' in Fig. 8(b). The complementary multiple hydrogen bonds formed between the amide units in PNIPAm and the A units in A-PEO-A were responsible for the greater values of G' and G'' for PNIPAm/A-PEO-A. In addition, the values of G' and G'' of the PNIPAm/A-PEO-A blends both increased gradually upon increasing the molar mass of A-PEO-A, reaching their maxima at around a molar ratio of 1:1 and decreasing thereafter. As listed in Table 2, the values of G' for the PNIPAm/A-PEO-A blends at various molar ratios were 727,000 Pa (1:0.4), 838,000 Pa (1:1), 371,000 Pa (1:2), and 131,000 Pa (1:4); the corresponding values of G'' were 158,000, 149,000, 91,400, and 29,800 Pa, respectively. These trends are closely related to the micellar morphologies of the PNIPAm/A-PEO-A blends in Figs. S5 and S6. For the PNIPAm/A-PEO-A blend at a molar ratio of 1:0.4, Fig. S5(b2) reveals a simple, vague, coarse network structure; at a molar ratio of 1:1, Fig. S5(c2) reveals a complex, clear, fine network structure

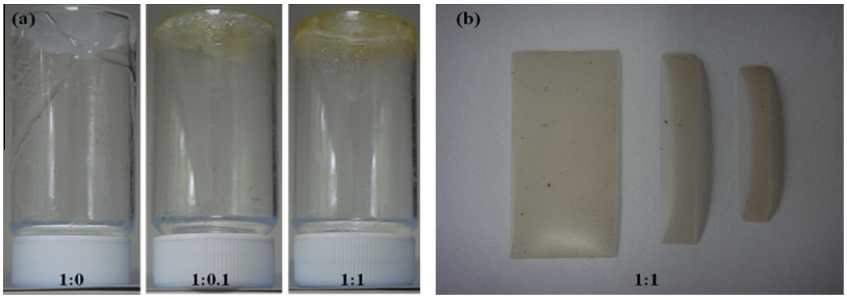

Fig. 7. (a) Gel phenomena of pure PNIPAm and PNIPAm/A-PEO-A blends at molar ratios of 1:0.1 and 1:1; (b) flexible films obtained from PNIPAm/A-PEO-A blends at a molar ratio of 1:1.

Table 2
Elastic modulus (G') and viscous modulus (G'') of PNIPAm/A-PEO-A supramolecular complexes at 25 °C.

PNIPAm/A-PEO-A	1:0	1:0.1	1:0.4	1:1	1:2	1:4	0:1
G' (Pa)	5960	10,400	24,800	664,000	636,000	390,000	120,500
G'' (Pa)	1840	4560	8190	188,000	149,000	86,300	25,600

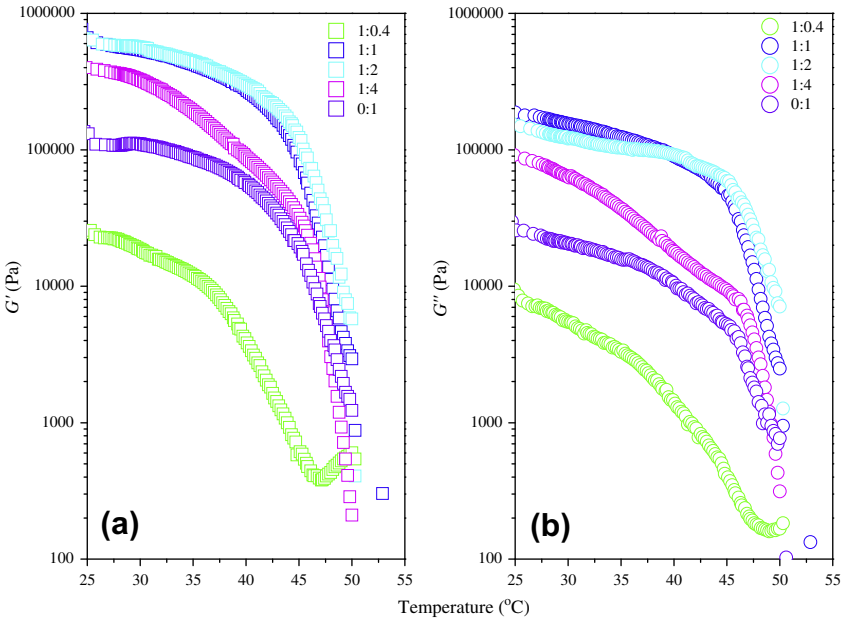

Fig. 8. Viscoelastic properties: (a) elastic modulus (G', □) and (b) viscous modulus (G'', ○) of PNIPAm/A-PEO-A blends at various molar ratios.

and Fig. S6(a2) reveals a core–shell toroidal structure; at a molar ratio of 1:4, Fig. S6(b2) reveals a core–shell–shell toroidal structure. The network structure had the largest positive effect on the values of G' and G'' of PNIPAm/A-PEO-A; the toroid structure followed, with the spherical micelles and large associated aggregates of spherical micelles having the weakest effects.

4. Conclusions

In this study, we prepared supramolecular complexes from PNIPAm/A-PEO-A blends in distilled water, stabilized through complementary multiple hydrogen bonds between the amide groups of PNIPAm and the A units in A-PEO-A. The presence of these structures improved the thermo-sensitive properties of the PNIPAm/A-PEO-A blends greatly, reaching an LCST of up to 40.3 °C. The PNIPAm/A-PEO-A blends also exhibited good film-forming properties, with a high degree of gelation, good toughness, elasticity, and flexibility.

Acknowledgement

This study was supported financially by the National Science Council, Taiwan, Republic of China, under contracts NSC 100-2221-E-110-029-MY3 and NSC 100-2628-E-110-001.

Appendix A. Supplementary material

Experimental detail of FTIR, GPC, and MALDI-TOF mass spectra of A-PEO-A and ^{1}H NMR, and GPC analyses of PNIPAm are available in supporting information.

Supplementary data associated with this article can be found, in the online version, at http://dx.doi.org/10.1016/j.eurpolymj.2013.10.023.

References

[1] Ahn SK, Kasi RM, Kim SC, Sharma N, Zhou Y. Soft Matter 2008;4:1151–7.
[2] Yan XZ, Wang F, Zheng B, Huang FH. Chem Soc Rev 2012;41:6042–65.
[3] Chopko CM, Lowden EL, Engler AC, Griffith LG, Hammond PT. ACS Macro Lett 2012;1:727–31.
[4] Yang HW, Chen JK, Cheng CC, Kuo SW. Appl Surf Sci 2013;271:60–9.
[5] Weiss J, Laschewsky A. Macromolecules 2012;45:4158–65.
[6] Trzebicka B, Robak B, Trzcinska R, Szweda D, Suder P, Silberring J, et al. Eur Polym J 2013;49:499–509.
[7] Kujawa P, Winnik FM. Macromolecules 2001;43:4130–5.
[8] Schmidt S, Motschmann H, Hellweg T, von Klitzing R. Polymer 2008;49:749–56.
[9] Xiong D, He ZP, An YL, Li Z, Wang H, Chen X, et al. Polymer 2008;49:2548–52.
[10] Man V, Silva ME, Barbani N, Giusti PJ. J Appl Polym Sci 2004;92:743–8.
[11] Li J, He WD, He N, Han SC, Sun XL, Li LY, et al. J Polym Sci Part A 2009;47:1450–62.
[12] Sun ST, Zhang WD, Zhang W, Wu PY, Zhu XL. Soft Matter 2012;8:3980–7.
[13] Liu XB, Luo SK, Ye J, Wu C. Macromolecules 2012;45:4830–8.
[14] Jin SP, Liu MZ, Chen SL, Gao CM. Eur Polym J 2008;44:2162–70.
[15] Fu HK, Kuo SW, Huang CF, Chang FC, Lin HC. Polymer 2009;50:1246–50.
[16] Zhang Y, Jiang M, Zhao J, Ren X, Chen D, Zhang G. Adv Funct Mater 2005;15:695–9.
[17] Luo YL, Yu W, Xu F, Zhang LL. J Polym Sci Part A 2012;50:2053–67.
[18] Ma XM, Xi JY, Xian Z, Tang XZ. J Polym Sci Part B 2005;43:3575–83.
[19] Di CF, Jiang XS, Yin J. Appl Polym Sci 2010;115:1831–40.
[20] Cao CW, Yang K, Wu F, Wei XQ, Lu LC, Cai YL. Macromolecules 2010;43:9511–21.
[21] Du HB, Qian XH. J Polym Sci Part B 2011;49:1112–22.
[22] Trongsatitkul T, Budhlall BM. Langmuir 2011;27:13468–80.
[23] You YZ, Zhou QH, Manickam DS, Wan L, Mao GZ, Oupicky D. Macromolecules 2007;40:8617–24.
[24] Li J, He WD, Han SC, Sun XL, Li LY, Zhang BY. J Polym Sci Part A 2009;47:786–96.

[25] Zhang BY, He WD, Li LY, Sun XL, Li WT, Zhang KR. J Polym Sci Part A 2010;48:3604–12.
[26] Li LY, He WD, Li WT, Zhang KR, Pan TT, Ding ZL, et al. J Polym Sci Part A 2010;48:5018–29.
[27] Scherzinger C, Lindner P, Keerl M, Richtering W. Macromolecules 2010;43:6829–33.
[28] Zhang WA, Wang SH, Li XH, Yuan JY, Wang SL. Eur Polym J 2012;48:720–9.
[29] Kuo SW, Hong JL, Huang YC, Chen JK, Fan SK, Ko FH, et al. J Nanomater 2012:749732.
[30] Tu CW, Kuo SW, Chang FC. Polymer 2009;50:2958–66.
[31] Mei AX, Guo XL, Ding YW, Zhang XH, Xu JT, Fan ZQ, et al. Macromolecules 2010;43:7312–20.
[32] Lai CT, Chien RH, Kuo SW, Hong JL. Macromolecules 2011;44:6546–56.
[33] Chen HW, Li JF, Ding YW, Zhang GZ, Zhang QJ, Wu C. Macromolecules 2005;38:4403–8.
[34] Chen HW, Zhang QJ, Li JF, Ding YW, Zhang GZ, Wu C. Macromolecules 2005;38:8045–50.
[35] Chen HW, Li WW, Zhao H, Gao JG, Zhang QJ. J Colloid Interface Sci 2006;298:991–5.
[36] Chen HW, Ye XD, Zhang GZ, Zhang QJ. Polymer 2006;47:8367–73.
[37] Yan JJ, Ji WX, Chen EQ, Li ZC, Liang DH. Macromolecules 2008;41:4908–13.
[38] Lee HN, Bai ZF, Newell N, Lodge TP. Macromolecules 2010;43:9522–8.
[39] Pollino JM, Weck M. Chem Soc Rev 2005;34:193–207.
[40] Yan XZ, Zhou M, Chen JZ, Chi XD, Dong SY, Zhang MM, et al. Chem Commun 2011;47:7086–8.
[41] Yan XZ, Xu DH, Chi XD, Chen JZ, Dong SY, Ding X, et al. Adv Mater 2012;24:362–9.
[42] Chen JZ, Yan XZ, Zhao QL, Li L, Huang FH. Polym Chem 2012;3:458–62.